

1    **Single Defect Center Scanning Near-Field Optical Microscopy on Graphene**  
2  
3

4    J. Tisler, T. Oeckinghaus, R. Stöhr, R. Kolesov, F. Reinhard and J. Wrachtrup

5    3. Institute of Physics, Stuttgart University, 70550 Stuttgart, Germany

9    **Abstract**

10   We demonstrate high resolution scanning fluorescence resonance energy transfer  
11   microscopy between a single nitrogen-vacancy center as donor and graphene as acceptor.

12   Images with few nanometer resolution of single and multilayer graphene structures were  
13   attained. An energy transfer efficiency of 30% at distances of 10nm between a single  
14   defect and graphene was measured. Further the energy transfer distance dependence of  
15   the nitrogen-vacancy center to graphene was measured to show the predicted  $d^{-4}$   
16   dependence. Our studies pave the way towards a diamond defect center based versatile  
17   single emitter scanning microscope.

18

19   **Introduction**

20   Imaging the optical near field of nano-sized structures is of fundamental interest to  
21   various areas of photonic-, material- and biological sciences.

22   As a result a wealth of scanning near-field optical microscopy (SNOM) techniques are  
23   available nowadays<sup>1</sup>. A notable extension to SNOM is scanning fluorescence resonance  
24   energy transfer microscopy<sup>2</sup>. The method exploits fluorescence resonance energy  
25   transfer (FRET)<sup>3</sup>, a non-radiative dipole-dipole interaction between transition dipole  
26   moments of a donor and an acceptor. As the method exploits the near field interaction of

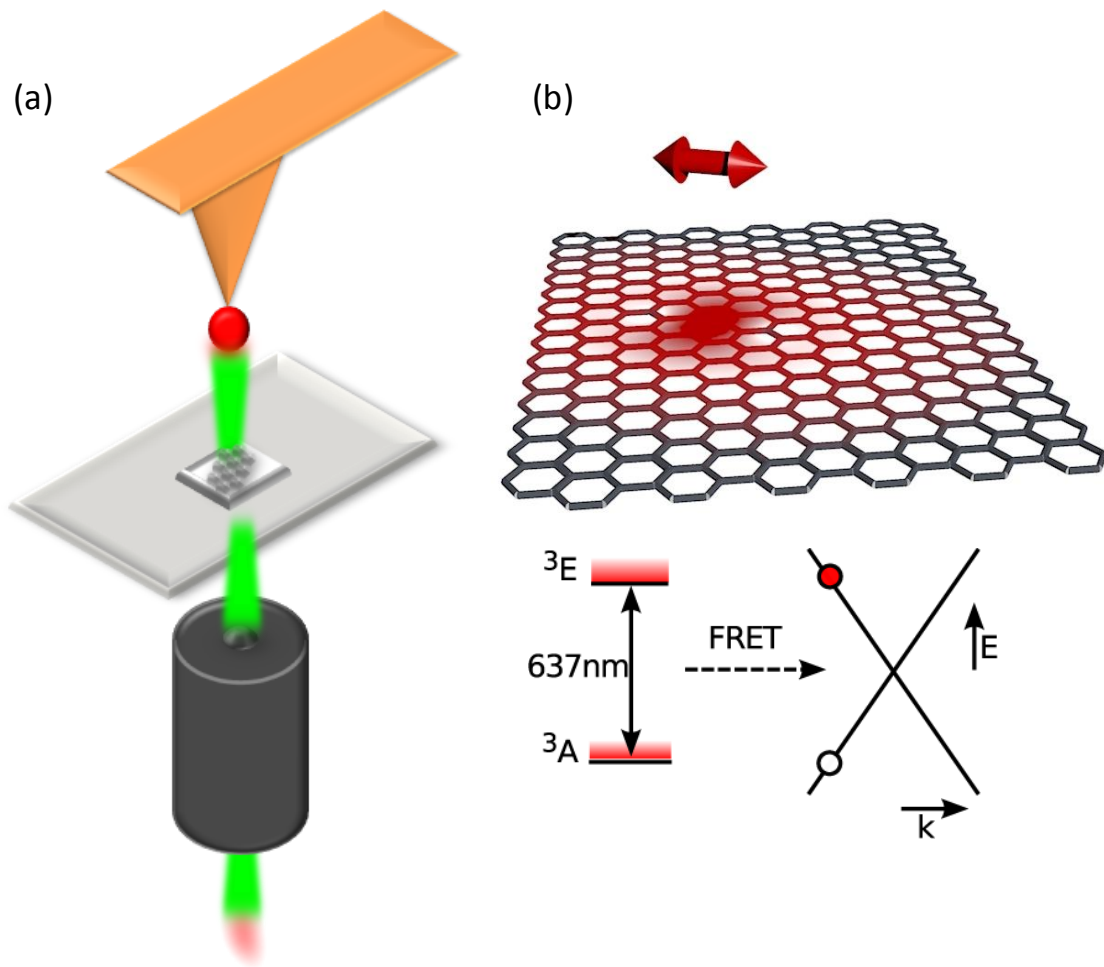
27 two induced dipoles it has a steep dependence on distance  $d$  ( $z^{-6}$ ) and promises to be  
28 capable of achieving nm resolution. Different donors and acceptor systems have been  
29 used like dyes<sup>4</sup>, color centers<sup>5</sup> or quantum dots<sup>6</sup>. But most of these systems suffer from  
30 blinking or limited photostability rendering their use cumbersome in practice. At low  
31 temperature single molecular fluorescence usually is stable and as a consequence  
32 scanning fluorescence imaging of light fields has been demonstrated<sup>7</sup>. One particular  
33 photoactive system, namely the nitrogen-vacancy (NV) center in diamond has gained  
34 attention as an atom-like photon emitter. It proves to be photostable even at room  
35 temperature<sup>8</sup>, can be brought into nm proximity of any photonic system<sup>9</sup> and has been  
36 proposed as a stable emitter for near-field microscopy<sup>4</sup>. As a result FRET has been  
37 demonstrated between a NV and another single molecule with high transfer efficiency  
38<sup>10,11</sup>. Therefore it appears to be an ideal emitter for FRET SNOM. In this study we utilize  
39 a scanning near field FRET microscope to investigate the interaction of a single NV  
40 emitter with graphene. Graphene has a number of intriguing near-field optical properties  
41 like high mode density<sup>12</sup> and it is speculated that graphene plasmons are easily launched  
42 by near field interactions with emitters. Further on only 2.3% of the incoming far field  
43 plane wave absorbed from a monolayer<sup>13</sup> making near and far field effects to be clearly  
44 distinguishable. Owing to its two dimensional geometry the distance dependence of the  
45 FRET efficiency is expected to be  $z^{-4}$  dependent<sup>14</sup> rather than  $z^{-6}$ . Additionally the FRET  
46 transfer efficiency probes relevant material properties like the local fermi energy.

47

48

49 **Results**

50 All the experiment use a home-build scanning FRET microscope based on an atomic  
51 force microscope (AFM) with an optically accessible tip. Single NV centers inside  
52 nanodiamonds on the tip of the AFM are used as FRET donors. A laser beam exciting the  
53 NV center is focused through the sample onto the NV. Fluorescence of the defect center  
54 is collected through the same channel (see Fig. 1).



55  
56 **Figure 1: Schematic images of the experiment** (a) Schematic image of the  
57 experimental setup. Nanodiamonds are glued onto the apex of a Si tip. A high  
58 numerical aperture objective (NA 1.3 is used to excite a single NV in the  
59 nanodiamond and collect NV fluorescence. (b) Energy levels of the lowest optical

60 transition relevant for energy transfer and and graphene band structure near the  $\Gamma$   
61 point.

62

63 To allow for close proximity between the defect and graphene small nanodiamond with  
64 diameters around  $\sim 25\text{nm}$  containing single NV centers were used. When the NV center  
65 is placed in close proximity to the graphene sample, its fluorescence is quenched by  
66 Förster energy transfer. In this process, an electronic excitation of the NV center is  
67 nonradiatively transferred into an exciton in graphene (Fig. 1b) which quickly dissipates  
68 excitation energy mostly by internal radiationless decay <sup>15</sup> ccuring at a rate  $\gamma_{nr}$ , this  
69 process competes with radiative emission of the NV center and reduces the fluorescence  
70 intensity to a value

$$I = \frac{\gamma_{ex}\gamma_r}{\gamma_r + \gamma_{nr}}$$

71 where  $\gamma_{ex}$  and  $\gamma_r$  are the excitation rate and radiative rate, respectively, and we assume  
72  $\gamma_{ex}$  to be much below saturation.

73 The quenching rate  $\gamma_{nr}$  can be computed from Förster's law<sup>16</sup> with the additional  
74 assumption that a sheet of graphene can be approximated by a two-dimensional array of  
75 infinitesimal flakes<sup>17</sup>.

$$\gamma_{nr} = A \iint_{\text{graphene}}_{\text{sheet}} ds^2 |\mathbf{E}_p|^2 \mu_g^2 = A \iint_{\text{graphene}}_{\text{sheet}} ds^2 \frac{\mu_{eg}^2 \mu_g^2 f(\hat{\mathbf{r}}, \widehat{\boldsymbol{\mu}_{eg}})}{r^6} \quad (1).$$

76 Here, A is a proportionality constant and  $\mathbf{E}_p = \mathbf{E} - (\mathbf{e}_z \cdot \mathbf{E})\mathbf{e}_z$  denotes the in-plane  
77 component of  $\mathbf{E} = (3\hat{\mathbf{r}}(\boldsymbol{\mu}_{eg} \cdot \hat{\mathbf{r}}) - \boldsymbol{\mu}_{eg})/(4\pi\epsilon_0 r^3)$ , the near-field of the transition  
78 dipole  $\boldsymbol{\mu}_{eg} = -e\langle e|\mathbf{r}|g\rangle$  of the NV center's optical transition between states  $|g\rangle$  and  $|e\rangle$   
79 (red shade in Fig. 1b). The graphene transition dipole moment  $\mu_g$  is a scalar, reflecting the

80 fact that graphene is an isotropic material. Hence, exciton transitions can be driven by  
81 any in-plane driving field  $\mathbf{E}_p = E \mathbf{e}_p$ , regardless of its polarization  $\mathbf{e}_p$ . Precisely,  
82  $ds^2 \mu_g^2 = e^2 \sum_{\mathbf{k}_i, \mathbf{k}_f, \omega = v_F(\mathbf{k}_f + \mathbf{k}_i)} |\langle \mathbf{k}_f | x | \mathbf{k}_i \rangle|^2$  where  $|\mathbf{k}_i\rangle, |\mathbf{k}_f\rangle$  denote plane-wave  
83 electron states in graphene and  $\omega$  is the NV transition's frequency.

84 Integrating equation (1) over an infinitely large graphene surface yields a modified  
85 Förster type law

$$\gamma_{nr} = \gamma_r \frac{z_0^4}{z^4}, \quad (2)$$

86 with a Förster distance  $z_0$  and a quenching rate rising with the fourth power of distance,  
87 differing markedly from the  $z^{-6}$  law commonly known for point like objects such as  
88 molecules or atoms.

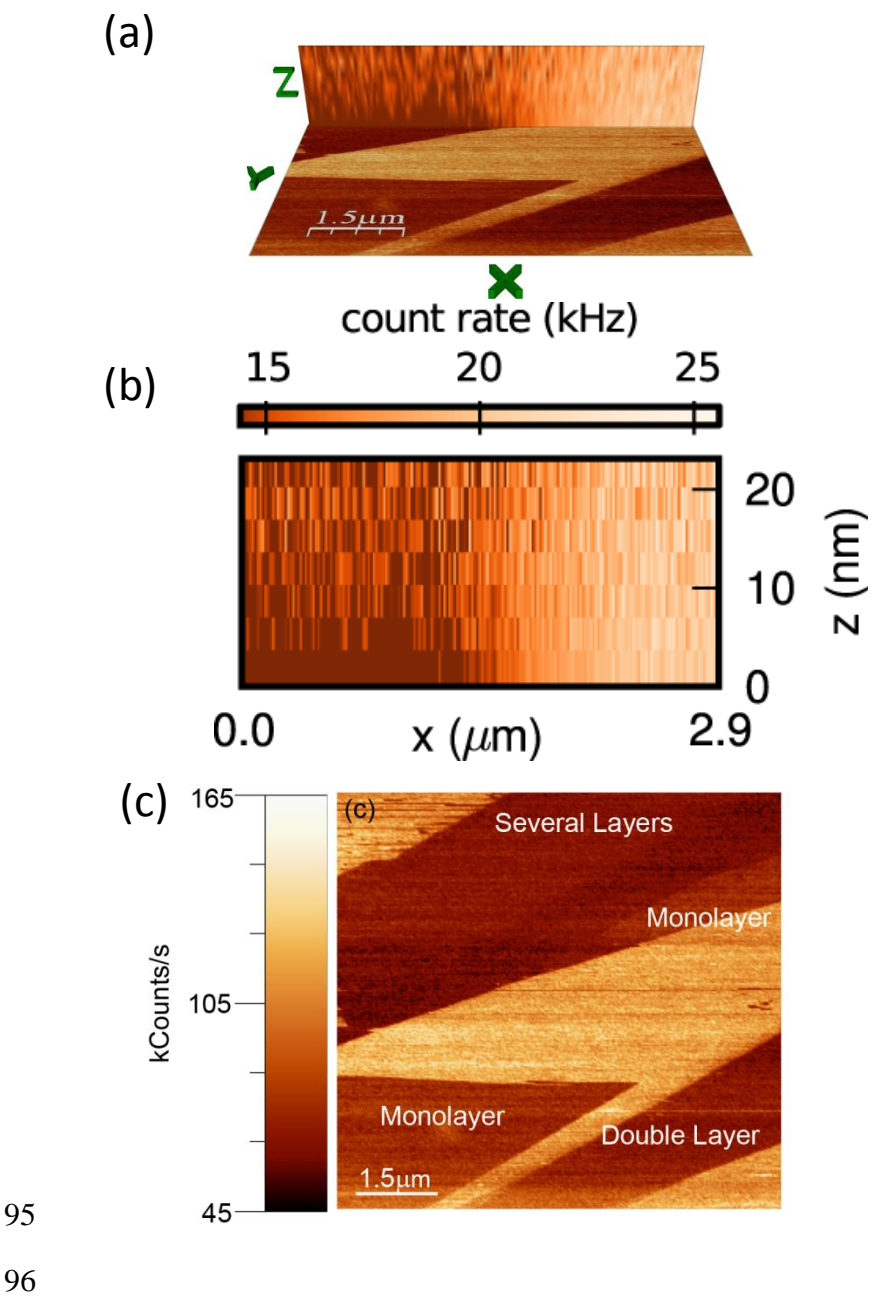
89 Quantitatively, the Förster distance can be calculated from eq. (2) and the expressions of  
90  $\gamma_{nr}$  and  $\gamma_r$  stated in previous work<sup>7 14</sup>.

$$z_0 = \sqrt[4]{\frac{9e^2 \hbar^3 c^3}{4.512 (\hbar \omega)^4 \epsilon_0}} = 15.3 \text{ nm.} \quad (3)$$

92

93

94



97 **Figure 2: Scanning FRET on graphene mono- and multiple layers. Plots show the**  
 98 **NV fluorescence intensity as a function of lateral (c) as well as lateral and axial**  
 99 **position over the graphene sample.**

100 In the following we discuss our scanning FRET experiments on layers of different  
 101 graphene thickness. It is worth mentioning that in addition to lateral xy scans we also

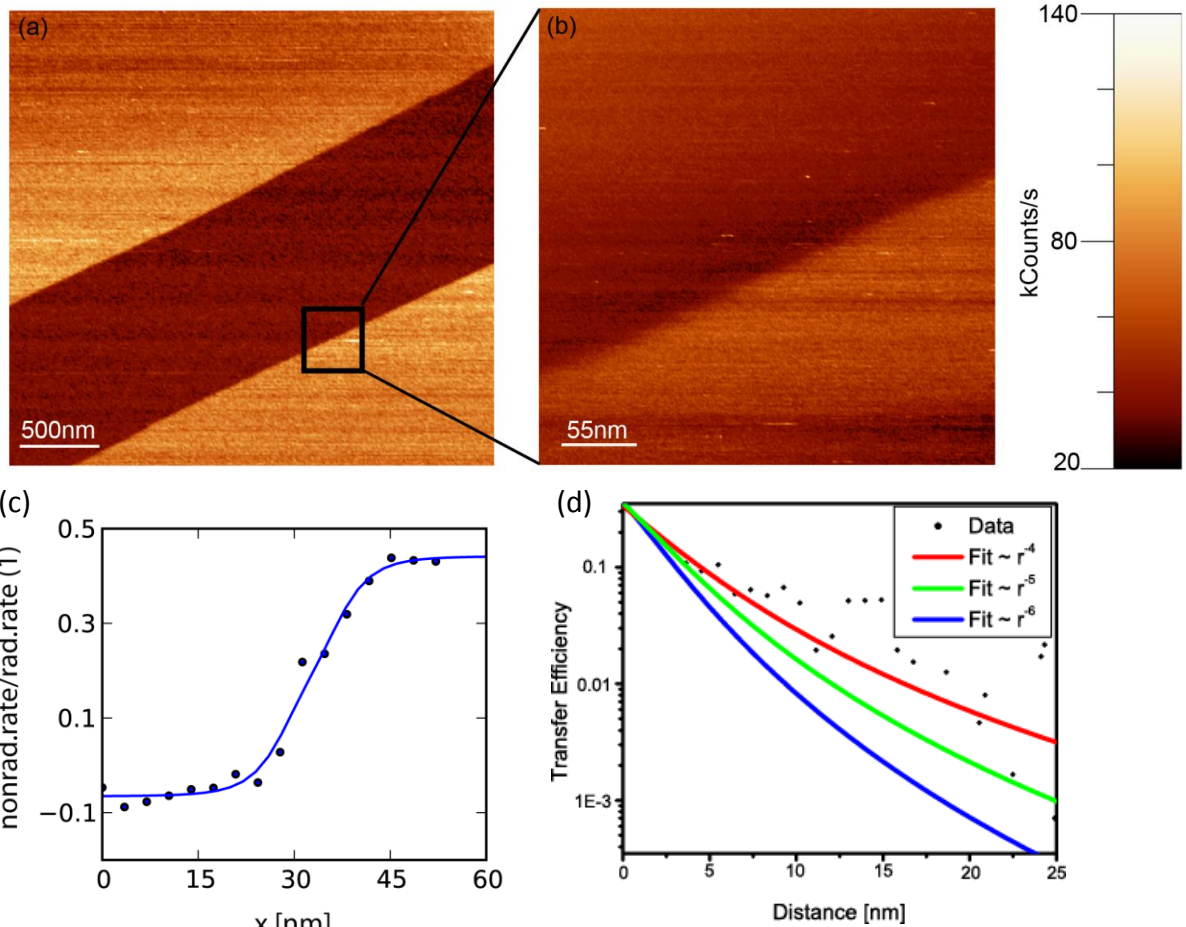
102 measured in xz- and in xy-direction. For such images tapping mode scanning FRET is  
103 used. In this mode the tip of the AFM is oscillating during scanning in contrast to contact  
104 mode. The photons arriving during the scan are measured in registry with the different  
105 heights of the oscillating tip.. Fig. 2b shows a corresponding image in the xz plane. To  
106 compare eq. (1) with results from Fig. 2c, we transform the fluorescence  
107  $I(x, y, z)$  observed in measurements into a quenching rate  $\gamma_{nr}(x, y, z)$  by the relation

108

$$\gamma_{nr} = \left( \frac{I_0}{I(x, y, z)} - 1 \right) \gamma_r, \quad (4)$$

109 where  $I_0$  is the unquenched NV fluorescence intensity. In all the following, we assume a  
110 radiative rate  $\gamma_r = 1/\tau_{NV}$  based on the measured fluorescence lifetime  $\tau_{NV} = 13\text{ns}^{18}$ .  
111 Note that this conversion implicitly assumes unity quantum efficiency.

112 In case of Fig. 2 the monolayer quenching rate was  $27.7\text{E}^6 \text{ s}^{-1}$  for a double layer  $33.1\text{E}^6 \text{ s}^{-1}$   
113 and for several layers  $46.2\text{E}^6 \text{ s}^{-1}$ . In contrast to previous work<sup>19</sup> no exact scaling with  
114 layer thickness was observed, probably due to background contributions which were not  
115 taken into account in our measurements.



116

117 **Figure 3: Quantitative comparison of scanning fluorescence resonance energy**  
 118 **transfer microscopy images to theory. A high resolution contact-mode scan of a**  
 119 **graphene edge (a-b) is used to measure the step response function of the single NV**  
 120 **center scanning over the graphene monolayer (c) The solid line of (c) is a fit to the**  
 121 **data using eq. (1), parametrized by the NV-graphene distance of  $z_{NV} = 9.8$  nm. (d)**  
 122 **Vertical dependence  $\gamma_{NV}(z)$ . A fit of the data (red line) agrees with the predicted**  
 123  **$z^{-4}$  law (eq. (2)) for a Förster distance of  $z_0 = 8.25 \pm 0.13$  nm.**

124

125 Thanks to their atomic size, scanning single emitters are able to map near-field couplings  
 126 with molecular (nm) resolution in all three dimensions. As a first application of this

127 remarkable property, we experimentally confirmed the theoretical model of eq. (1). The  
 128 result is shown in Fig. 3. In the lateral dimensions (Fig. 3 a-c), a high-resolution scan of a  
 129 graphene edge (Fig. 3b) reveals that fluorescence drops smoothly over a length scale of  
 130 ~10nm when the NV center is moved over the flake. The theoretical prediction (solid line  
 131 in Fig. 3c) is obtained by numerically integrating equation (1), taking into account the  
 132 fact that the NV transition has two orthogonal transition dipoles  $\mu_1, \mu_2$

$$\gamma_{nr}(x) = (\gamma_{nr}^{\mu_1}(x) + \gamma_{nr}^{\mu_2}(x))/2$$

$$\gamma_{nr}^{\mu}(x) = A\mu_g^2 \int_x^{\infty} dx \int_{-\infty}^{\infty} dy |\mathbf{E}_p^{z_{NV}, \mu}(x, y)|^2.$$

133 The remaining free parameters  $A, \mu_g^2$  and  $z_{NV}$  are fit to the data and the dipole  
 134 orientation is chosen as  $\mu_1 \parallel e_z, \mu_2 \parallel e_x$  to best fit the observed behaviour. We find that  
 135 the data agrees well with the theoretical prediction (Fig. 3c). The achieved resolution is  
 136 limited by the spatial extent of the near-field  $\mathbf{E}_p$ , which is of the order of the NV-  
 137 graphene distance. Reverting the argument, we can extract this distance from the fit,  
 138 finding that  $z_{NV} = 9.8$  nm. This value is nonzero even though the nanodiamond was  
 139 scanned over the graphene in contact mode. Therefore, we interpret this value as the  
 140 distance between the NV center and the surface of the nanodiamond.

141 We also measured the vertical dependence  $\gamma_{nr}(z)$  by repeatedly approaching and  
 142 retracting the tip on a large graphene surface (Fig 3d). Again, we find that the data is well  
 143 described by eq. (1) and in particular agrees with the predicted  $z^{-4}$  law of eq. (2). Using  
 144 the value  $z_{NV}$  obtained from the lateral scan, we can quantitatively fit the data and infer a  
 145 Förster distance of  $z_0 = 8.25 \pm 0.13$  nm . This differs significantly from the theory  
 146 prediction ( $z_0 = 15.3$  nm, eq. (3)). Most likely, this difference is due to additional

147 nonradiative channels which lower the NV center's quantum efficiency and thus reduce  
148  $z_0$ . The existence of such channels is likely and candidates include quenching by the  
149 silicon AFM tip or an intrinsically low quantum efficiency in nanodiamonds. Conversely,  
150 we note that our result provides a method to measure the quantum efficiency of a single  
151 emitter when it is combined with a quantitative theory of excitonic transitions in  
152 graphene<sup>1420</sup>.

153

154 **Conclusion**

155 We demonstrated optical scanning fluorescence resonance energy transfer microscopy  
156 with a single NV center in nanodiamond as emitter. By scanning over a graphene  
157 monolayer we attained nanometer resolution images and a transfer efficiency as large as  
158 30%. Furthermore we experimentally confirmed a  $z^4$  dependence of the energy transfer  
159 rate between a point-like emitter and a graphene monolayer. While graphene is an  
160 interesting photonic material in its own right, application of the technique to other nano  
161 photonic structures and acceptors, e.g. single molecules certainly would be of great  
162 interest. Applications in biological sciences where scanning FRET might become a  
163 valuable addition to other FRET based techniques for, e.g. imaging larger protein  
164 structures of cellular surfaces are easily envisioned. Such methods may be combined with  
165 the magnetic field sensing capabilities of the NV center to yield a truly multifunctional  
166 local probe.

167

168

169 **Acknowledgement**

170 Financial support by the EU via projects SQUTEC and DINAMO as well as the German  
171 Science foundation via research group 1493 and SFB/TR 21 is acknowledged.

172

173 **References**

- 174 1. Betzig, E., Trautman, J. K., Harris, T. D., Weiner, J. S. & Kostelak, R. L. Breaking  
175 the Diffraction Barrier: Optical Microscopy on a Nanometric Scale. *Science* **251**,  
176 1468–1470 (1991).
- 177 2. Sekatskii, S. K. & Letokhov, V. S. Nanometer-resolution scanning optical  
178 microscope with resonance excitation of the fluorescence of the samples from a  
179 single-atom excited center. *Jetp Lett.* **63**, 319–323 (1996).
- 180 3. Lakowicz, J. R. *Principles of fluorescence spectroscopy*. (Springer: 2006).
- 181 4. Gruber, A. *et al.* Scanning Confocal Optical Microscopy and Magnetic Resonance on  
182 Single Defect Centers. *Science* **276**, 2012–2014 (1997).
- 183 5. Shubeita, G. T. *et al.* Scanning near-field optical microscopy using semiconductor  
184 nanocrystals as a local fluorescence and fluorescence resonance energy transfer  
185 source. *J Microsc* **210**, 274–278 (2003).
- 186 6. Y. Ebenstein, T. M. Quantum-Dot-Functionalized Scanning Probes for Fluorescence-  
187 Energy-Transfer-Based Microscopy. (2003).doi:10.1021/jp036135j
- 188 7. Michaelis, J. *et al.* A single molecule as a probe of optical intensity distribution. *Opt.  
189 Lett.* **24**, 581–583 (1999).
- 190 8. Michalet, X. *et al.* Quantum Dots for Live Cells, in Vivo Imaging, and Diagnostics.  
191 *Science* **307**, 538 –544 (2005).
- 192 9. Kurtsiefer, C., Mayer, S., Zarda, P. & Weinfurter, H. Stable Solid-State Source of  
193 Single Photons. *Phys. Rev. Lett.* **85**, 290–293 (2000).
- 194 10. Tisler, J. *et al.* Highly Efficient FRET from a Single Nitrogen-Vacancy Center in  
195 Nanodiamonds to a Single Organic Molecule. *ACS Nano* **5**, 7893–7898 (2011).
- 196 11. Kühn, S., Hettich, C., Schmitt, C., Poizat, J.-P. & Sandoghdar, V. Diamond colour  
197 centres as a nanoscopic light source for scanning near-field optical microscopy.  
198 *Journal of Microscopy* **202**, 2–6 (2001).
- 199 12. Koppens, F. H. L., Chang, D. E. & García de Abajo, F. J. Graphene Plasmonics: A  
200 Platform for Strong Light-Matter Interactions. *Nano Letters* (2011).at  
201 <<http://resolver.caltech.edu/CaltechAUTHORS:20110929-105946388>>
- 202 13. Nair, R. R. *et al.* Fine Structure Constant Defines Visual Transparency of Graphene.  
203 *Science* **320**, 1308–1308 (2008).
- 204 14. Swathi, R. S. & Sebastian, K. L. Long range resonance energy transfer from a dye  
205 molecule to graphene has (distance)<sup>-4</sup> dependence. *The Journal of Chemical Physics*  
206 **130**, 086101–086101–3 (2009).

- 207 15. Stöhr, R. J., Kolesov, R., Pflaum, J. & Wrachtrup, J. Fluorescence of laser-created  
208 electron-hole plasma in graphene. *Phys. Rev. B* **82**, 121408 (2010).
- 209 16. Förster, T. Zwischenmolekulare Energiewanderung und Fluoreszenz. *Annalen der  
210 Physik* **437**, 55–75 (1948).
- 211 17. Stöhr, R. J. *et al.* Super-resolution Fluorescence Quenching Microscopy of Graphene.  
212 *ACS Nano* **6**, 9175–9181 (2012).
- 213 18. Robledo, L., Bernien, H., Sar, T. van der & Hanson, R. Spin dynamics in the optical  
214 cycle of single nitrogen-vacancy centres in diamond. *New Journal of Physics* **13**,  
215 025013 (2011).
- 216 19. Chen, Z., Berciaud, S., Nuckolls, C., Heinz, T. F. & Brus, L. E. Energy Transfer from  
217 Individual Semiconductor Nanocrystals to Graphene. *ACS Nano* **4**, 2964–2968  
218 (2010).
- 219 20. Swathi, R. S. & Sebastian, K. L. Resonance energy transfer from a dye molecule to  
220 graphene. *The Journal of Chemical Physics* **129**, 054703 (2008).
- 221
- 222
- 223